Environ. Sci. Technol. **2007**, *41,* 7661−7667

Nitrogen Isotopes as Indicators of NO_x Source Contributions to Atmospheric Nitrate Deposition Across the Midwestern and Northeastern United States

E. M. ELLIOTT,*,†,‡ C. KENDALL,† S. D. WANKEL,† D. A. BURNS,§ E. W. BOYER,|| K. HARLIN,⊥ D. J. BAIN,† AND T. J. BUTLER#

U.S. Geological Survey, Water Resources Division, 345 Middlefield Road, Menlo Park, California 94025, University of Pittsburgh, Department of Geology and Planetary Science, 4107 O'Hara Street, Pittsburgh, Pennsylvania 15260-3332, U.S. Geological Survey, New York Water Science Center, 425 Jordan Road, Troy, New York 12180, Department of Environmental Science, Policy & Management, 137 Mulford Hall, University of California, Berkeley, California 94720, National Atmospheric Deposition Program Central Analytical Lab, Illinois State Water Survey, 2204 Griffith Drive, Champaign, Illinois 61820-7495, Institute of Ecosystem Studies, Box AB, Millbrook, New York 12545-0129, and Department of Ecology and Evolutionary Biology, Cornell University, Ithaca, New York 12545-0129

Global inputs of NO_x are dominated by fossil fuel combustion from both stationary and vehicular sources and far exceed natural NO_x sources. However, elucidating NO_x sources to any given location remains a difficult challenge, despite the need for this information to develop sound regulatory and mitigation strategies. We present results from a regional-scale study of nitrogen isotopes ($\delta^{15}N$) in wet nitrate deposition across 33 sites in the midwestern and northeastern U.S. We demonstrate that spatial variations in $\delta^{15}N$ are strongly correlated with NO_x emissions from surrounding stationary sources and additionally that $\delta^{15}N$ is more strongly correlated with surrounding stationary source NO_x emissions than pH, SO_4^{2-}, or NO_3^- concentrations. Although emission inventories indicate that vehicle emissions are the dominant NO_x source in the eastern U.S., our results suggest that wet NO_3^- deposition at sites in this study is strongly associated with NO_x emissions from stationary sources. This suggests that large areas of the landscape potentially receive atmospheric NO_y deposition inputs in excess of what one would infer from existing monitoring data alone. Moreover, we determined that spatial patterns in $\delta^{15}N$ values are a robust indicator of stationary NO_x contributions to wet NO_3^- deposition and hence a valuable complement to existing tools for assessing relationships between NO_3^- deposition, regional emission inventories, and for evaluating progress toward NO_x reduction goals.

Introduction

Global atmospheric emissions of nitrogen oxide (NO_x, the sum of NO and NO_2) have increased dramatically during the past 150 years (*1*). Consequently, high rates of NO_x emissions and associated atmospheric deposition of nitrate (NO_3^-) pose threats to global ecosystems and human health (*2*, *3*). Contemporary global emissions of NO_x are dominated by fossil fuel combustion (63%) from both stationary (e.g., power plant electricity generation) and mobile (e.g., vehicular) sources and far exceed natural NO_x sources such as lightning, biogenic soil processes, and wildfires (*4*).

Given increased regulation of sulfur dioxide (SO_2) emissions in North America and Europe, NO_3^- is an increasingly important component of acidic deposition. In particular, in the northeastern U.S., sulfate (SO_4^{2-}) to NO_3^- ratios in atmospheric wet deposition have decreased sharply since the 1970s (*5*); thus, the effects of acid precipitation are now nearly as strongly driven by NO_3^- deposition as that of SO_4^{2-} (*6*). These effects include surface water and soil acidification, forest decline, impaired air quality, and coastal eutrophication (*7*). To address these effects, new regulations increasingly target NO_x reductions in the U.S. (2005 Clean Air Interstate Rule) and Europe (2005 CAFÉ Programme-Thematic Strategy on Air Pollution). Elucidating NO_x sources to any given location is challenging, although such information is needed to develop sound regulatory, management, and mitigation strategies for air and water quality.

Once released to the atmosphere, NO_x oxidizes to nitric acid (HNO_3) through several potential pathways. Highly soluble and subject to scavenging in precipitation, HNO_3 is a major sink for NO_x. During the daytime, oxygen atoms rapidly exchange between O_3 and NO (eqs 1 and 2), and photolytic production of OH results in the oxidation of NO_2 to HNO_3 via the OH radical (eq 3)

$$NO + O_3 \rightarrow NO_2 + O_2 \quad (1)$$

$$NO_2 + h\nu \rightarrow NO + O \quad (2)$$

$$NO_2 + OH \rightarrow HNO_3 \quad (3)$$

During the nighttime, NO_2 is oxidized by O_3 to produce the nitrate radical (NO_3^-) (eq 4), which subsequently oxidizes to dinitrogen pentoxide (N_2O_5) (eq 5). Hydrolysis of N_2O_5 forms HNO_3 (eq 6)

$$NO_2 + O_3 \rightarrow NO_3 + O_2 \quad (4)$$

$$NO_3 + NO_2 \rightarrow N_2O_5 \quad (5)$$

$$N_2O_5 + H_2O \rightarrow 2HNO_3 \quad (6)$$

$\delta^{15}N$ values for anthropogenic and natural NO_x sources vary over a large range. $\delta^{15}N$ values of NO_x from coal-fired power plants range from +6 to +13‰ (*8*, *9*), whereas vehicle NO_x emissions in tailpipe exhaust, roadside denuders, and roadside vegetation have lower $\delta^{15}N$ values (+3.7, +5.7, and +3.8‰, respectively) (*10*−*12*), although negative $\delta^{15}N$ values in tailpipe exhaust have also been reported (−13 to −2‰) (*8*). $\delta^{15}N$ values from natural NO_x sources, including lightning, biogenic NO_x emissions, and biomass burning, have not been

* Corresponding author phone: (412)624-8882; fax: (412)624-3914; e-mail: eelliott@pitt.edu.
† U.S. Geological Survey, Menlo Park.
‡ University of Pittsburgh.
§ U.S. Geological Survey, Troy.
|| University of California, Berkeley.
⊥ National Atmospheric Deposition Program Central Analytical Lab.
Institute of Ecosystem Studies and Cornell University.

10.1021/es070898t CCC: $37.00
Published on Web 10/20/2007

directly characterized; however, low $\delta^{15}N$ values have been reported for NO_x produced during electrical discharges used to simulate lightning (−0.5 to +1.4‰) (*13*). Although $\delta^{15}N$ of biogenic NO_x has not been directly measured, lower $\delta^{15}N$ values observed at pristine sites relative to polluted sites (*10*, *11*), and lower $\delta^{15}N$ values observed during spring and summer relative to other seasons (*14*, *15*), suggest that negative fractionations accompany the release of biogenic NO_x. However, high $\delta^{15}N$ values of pre-industrial nitrate from ice cores suggest the possibility of a natural NO_x source characterized by high $\delta^{15}N$ values (*16*, *17*). While additional research is needed to refine $\delta^{15}N$ values from NO_x sources, the studies described are the best available and therefore were used for interpretation of our results.

Although precipitation NO_3^- isotopes have been characterized in localized areas (*18*), regional-scale analyses have been precluded by the difficulty of analyzing low concentration precipitation samples using conventional methods (*19*). Here, we present advances in fingerprinting NO_x sources that contribute to wet NO_3^- deposition across regional landscapes. This is the first large-scale study of precipitation NO_3^- isotopes, where we applied recently developed techniques (*20*, *21*) to investigate whether $\delta^{15}N$ values of precipitation NO_3^- can be used to distinguish dominant sources of NO_x to NO_3^- deposition in the midwestern and northeastern U.S.

Experimental Procedures

We analyzed archived precipitation collected at 33 National Atmospheric Deposition Program (NADP) National Trends Network (NTN) sites spanning the midwestern and northeastern U.S. The NTN monitors precipitation chemistry at over 250 sites in representative ecoregions across the U.S. to characterize regional patterns of atmospheric deposition. We chose 33 NTN sites that span a NO_3^- deposition gradient across the midwestern and northeastern U.S. bounded by Ohio, West Virginia, Pennsylvania, and Maine (Supporting Information Table SI-1). This region encompasses the large eastern population centers of New York City, Philadelphia, and Boston and large energy production facilities in the Ohio River Valley. We determined using an urban−rural classification system (*22*) that 2, 15, 16, and 1 sites are in urban, suburban, exurban, and rural counties, respectively. This classification suggests that data from these NTN sites should reflect a mixture of sources typical of suburban and rural environments. This arises from the deliberate location of NTN sites away from point and local sources of pollution, including transportation corridors, agricultural fields, livestock operations, and industrial emissions to most effectively represent regional deposition patterns (*23*).

Archived weekly samples of wet-only deposition collected during 2000 were pooled into volume-weighted bimonthly composite samples (e.g., January-February, March-April, etc.). These weekly samples were filtered (0.45 μm Gelman polyethersulfone filter), and NO_3^- concentrations were measured by ion chromatography (Dionex DX-500) at the time of initial collection (*24*). When the precipitation volume was sufficient, samples were archived at 4 °C at the NADP Central Analytical Laboratory in Champaign, IL. To test whether archived samples were suitable for isotopic analysis, a suite of 28 samples with a range of NO_3^- and ammonium (NH_4^+) concentrations was reanalyzed in 2003. Results show minimal alteration of NO_3^- concentrations (slope = 1.008, $r^2 = 0.9995$, and $p < 0.001$) and no significant relationship between NH_4^+ concentration and the percentage change in NO_3^- concentration. Although we cannot rule out potential fractionation during sample storage, the strong correlations between concentrations in 2000 and 2003, coupled with our observations of a large range in $\delta^{15}N$ values and consistent seasonal and spatial patterns, suggest that if fractionations occur, their effects on the isotopic composition of the sample solution is minimal.

A denitrifying bacteria, *Pseudomonas aureofaciens*, was used to convert 20−60 nmol of NO_3^- into gaseous N_2O prior to isotope analysis (*20*, *21*). Samples were analyzed for $\delta^{15}N$ in duplicate using a GV Instruments IsoPrime Continuous Flow Isotope Ratio Mass Spectrometer (CF-IRMS; use of brand names is for identification purposes only and does not imply endorsement by the U.S. Government), and values are reported in parts per thousand relative to atmospheric N_2 as follows:

$$\delta^{15}N\ (‰) = \frac{(^{15}N/^{14}N)_{sample} - (^{15}N/^{14}N)_{standard}}{(^{15}N/^{14}N)_{standard}} 1000 \qquad (7)$$

Samples were corrected using international reference standards USGS34 and N3; linearity and instrument drift were corrected using internal standards. $\delta^{15}N$ values were also corrected for mass independent contributions of ^{17}O to the m/z 45 signal of N_2O (*20*, *21*, *25*) by independently quantifying $\Delta^{17}O$ in a subset of bimonthly samples from 11 of the 33 sites across the study region ($n = 66$) (*26*). A correction factor was calculated based on measurements of $\Delta^{17}O$ and applied to all analyses, resulting in a mean correction of −1.5‰ ($n = 196$). Although $\Delta^{17}O$ contributions lowered $\delta^{15}N$ values and slightly dampened seasonal differences, they did not change spatial patterns. Sample replicates had an average standard deviation (σ) of 0.2‰ for $\delta^{15}N$ ($n = 196$). Analytical precision is 0.3‰ based on an internal reference standard that was analyzed at least once per 40 samples. $\delta^{15}N$ values were interpolated across the region using inverse distance weighting with a variable search radius.

To compare $\delta^{15}N$ values with potential emission sources, county-level, monthly emissions data from vehicles and electric generating units (EGUs) from the year 2000 were obtained from the U.S. EPA Emission Factors and Inventory Group and summed into bimonthly emissions. County-level estimates of vehicle NO_x emissions were compared to $\delta^{15}N$ values in counties where NTN sites are located; a larger source area was not considered based on studies that suggest local deposition of vehicle NO_x (*27*, *28*). Spatial patterns in stationary source NO_x emissions were assessed using monthly EGU NO_x emissions; these emissions are dominated by coal combustion, with lesser contributions from natural gas and oil, and comprise 25% of the total NO_x emissions in the eastern U.S. Stationary source emissions within various radial distances (50−800 km) around individual NTN sites were compiled using ArcMap. EGU NO_x emissions in counties within or intersecting these buffer areas were summed into bimonthly totals and normalized to emissions densities using county areas within or intersecting each source region. Although the predominant wind direction in this region is generally westerly, we used radial source areas to more completely consider all precipitation events that might contribute NO_3^- to individual sites. Canadian NO_x emissions were not considered in this study as they are generally <10% of NO_x emissions in the eastern U.S. (*29*).

Results

Across the region, bimonthly $\delta^{15}N$ values ranged from +3.2 to −8.1‰ (mean = −1.5‰ and $n = 196$), a range that is lower than $\delta^{15}N$−NO_x values from stationary sources (+6 to +13‰ and $n = 11$) (*8*, *9*) and lower than most studies of tailpipe exhaust, roadside denuders, and roadside vegetation (+3.7, +5.7, and +3.8‰, respectively) (*10*−*12*). Values were generally higher in the western states than in the eastern states (Figure 1). For example, $\delta^{15}N$ values in Ohio were

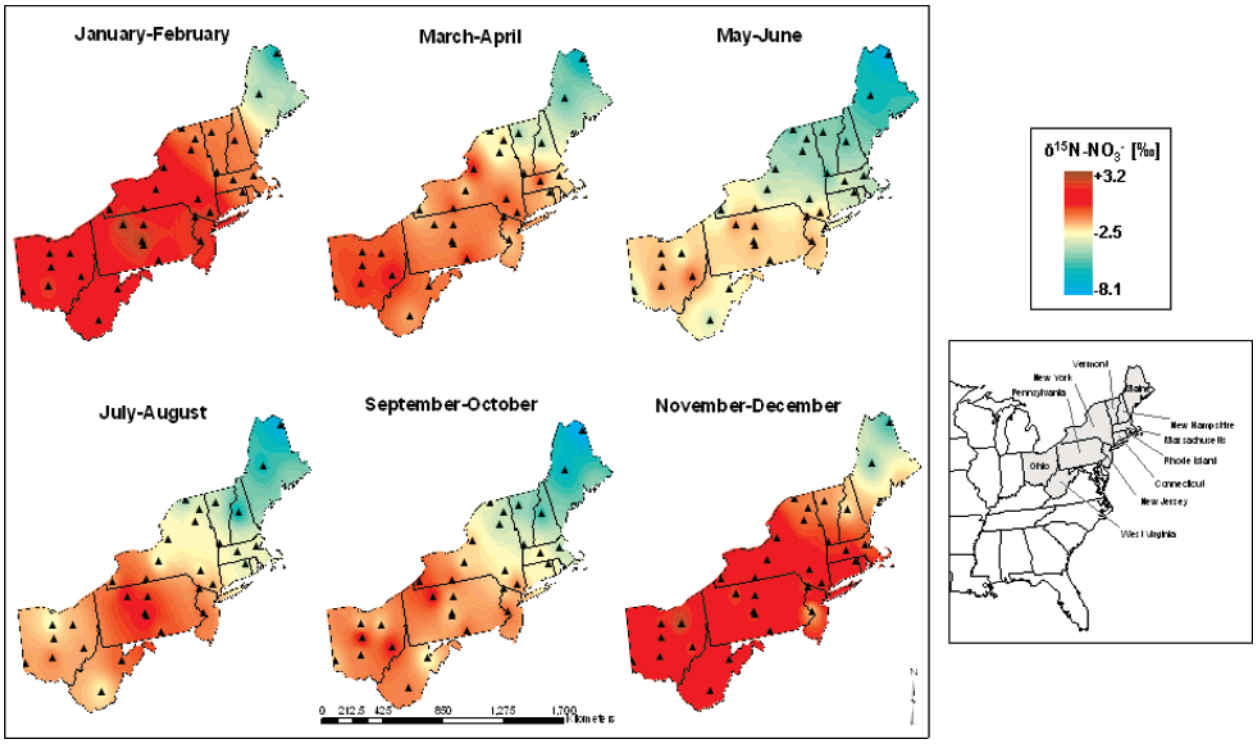

FIGURE 1. Bimonthly, volume-weighted $\delta^{15}N$ values of precipitation NO_3^- for 33 NTN sites in the midwestern and northeastern U.S.

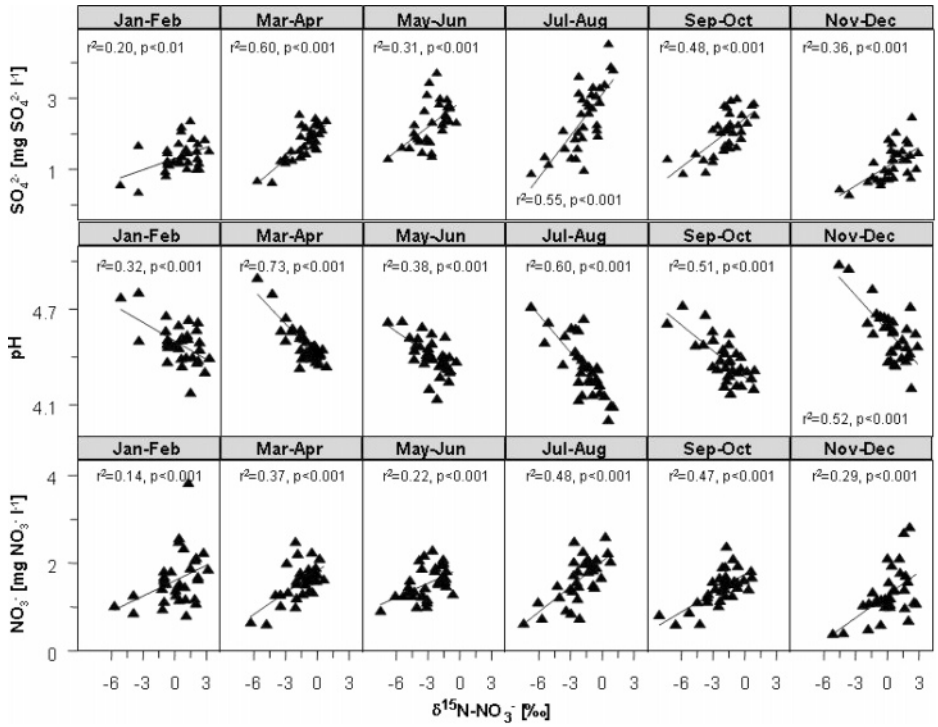

FIGURE 2. Bimonthly $\delta^{15}N$ values of precipitation NO_3^- vs volume-weighted, bimonthly SO_4^{2-} concentrations, pH, and NO_3^- concentrations for respective sites. For all plots, $n = 33$.

significantly higher than those in the three easternmost states (one-tailed t-test, $p < 0.0001$, $\alpha = 0.05$, and $n = 64$). The highest $\delta^{15}N$ value (+3.2‰) was observed at PA15 during January-February, and the lowest $\delta^{15}N$ value (−8.1‰) was observed at ME00 during September-October. The spatial gradient in $\delta^{15}N$ values was most pronounced during the winter months (Figure 1); however, even during July-August, $\delta^{15}N$ values spanned 8‰.

We also observed consistent seasonal trends across the sites where $\delta^{15}N$ values were significantly higher during colder months (November-April) than during warmer months (May-October) (one-tailed t-test, $p < 0.0001$, $\alpha = 0.05$, and $n = 196$) (Figure 1). Mean $\delta^{15}N$ values were 2.3‰ higher during January-February than during July-August for all sites.

Bimonthly $\delta^{15}N$ values were positively correlated with bimonthly, volume-weighted SO_4^{2-} and NO_3^- concentrations and negatively correlated with pH for all bimonths (Figure 2). $\delta^{15}N$ values were not correlated with bimonthly precipitation volume for any individual bimonth.

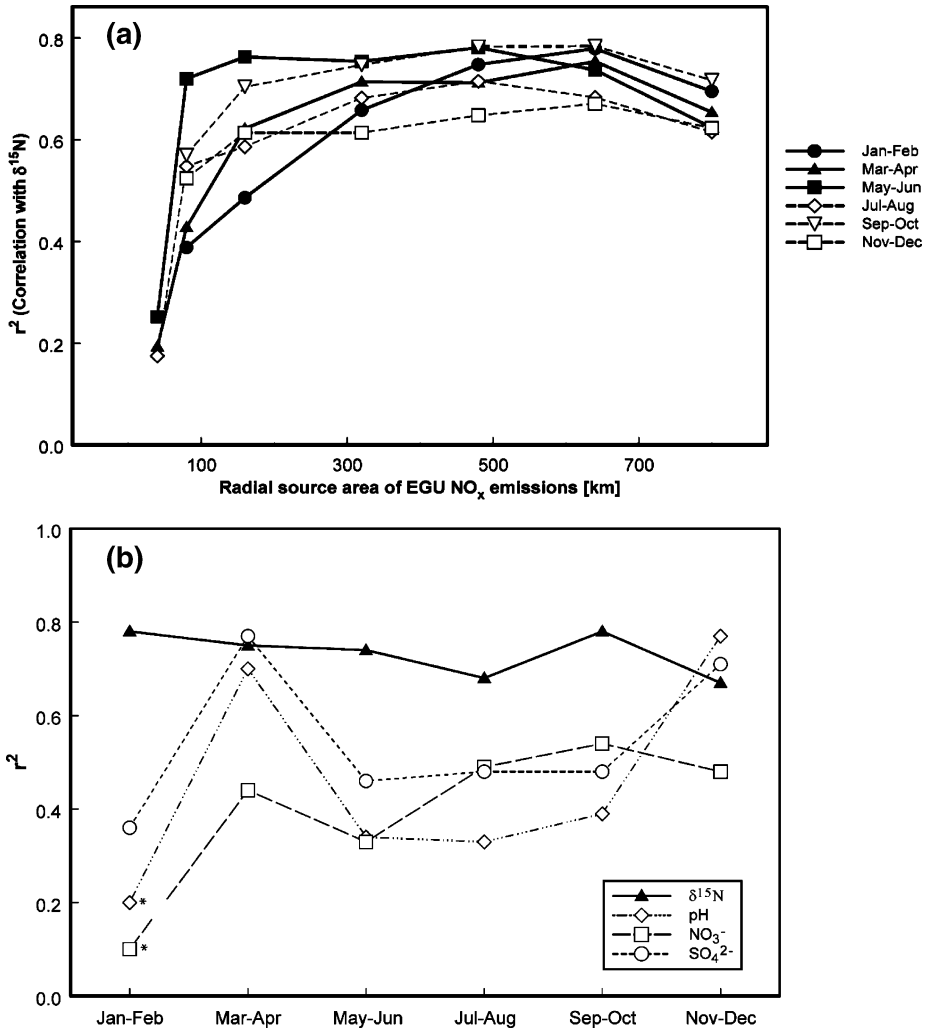

FIGURE 3. (a) Correlations between $\delta^{15}N$ and EGU NO_x emissions summed within varying radial source areas of NTN sites. Each point represents an r^2 value between bimonthly $\delta^{15}N$ values and EGU NO_x emissions density for a specific radial source area around NTN sites. (b) Bimonthly correlations between $\delta^{15}N$, pH, NO_3^- concentration, SO_4^{2-} concentration, and EGU NO_x emissions within 640 km of NTN sites. For each data point, $n = 33$ and $p < 0.001$ except where non-significant correlations are indicated by an asterisk.

Discussion

Although fractionations between NO_x derived from fossil fuel combustion (−13 to +13‰) and NO_3^- in wet deposition (−8.1 to +3.2‰) seem likely, we demonstrate using (i) precipitation chemistry; (ii) NO_x emissions data; and (iii) conceptualized mixing models that $\delta^{15}N$ in wet NO_3^- deposition nonetheless reflects the influence of stationary source NO_x emissions. Additionally, we consider potential fractionations during various oxidation reactions.

Precipitation Chemistry. Precipitation SO_4^{2-} concentrations in the eastern U.S. are strongly influenced by SO_2 emissions from stationary EGUs in the midwestern U.S. (*30*, *31*). The significant positive correlations observed between $\delta^{15}N$, NO_3^-, and SO_4^{2-} concentrations and the negative correlations with precipitation pH (Figure 2) suggest that $\delta^{15}N$ values reflect stationary source NO_x. In particular, county-level EGU NO_x emissions are substantially higher in the Ohio River Valley (Supporting Information Figure SI-1), and $\delta^{15}N$ values are generally highest east of these major emissions sources (Figure 1). $\delta^{15}N$ values are not correlated with precipitation volume; this suggests that $\delta^{15}N$ variability is not due to regional rainfall patterns.

Surrounding Stationary Source NO_x Emissions. We observe significant correlations between $\delta^{15}N$ values and EGU NO_x emissions within source areas of 80−800 km ($0.39 < r^2 < 0.78$, $p < 0.001$, and $n = 33$) (Figure 3a). The strongest correlations between $\delta^{15}N$ and EGU NO_x occur between ~500−600 km ($0.67 < r^2 < 0.78$) (Figure 3a), consistent with distances estimated from the U.S. EPA's Regional Acid Deposition Model (RADM) (400−600 km) (*32*) and from 12 and 24 h daily back trajectories for individual NTN sites (500−1000 km) (*29*). These strong correlations indicate that these NTN sites reflect regional transport of NO_x generated by EGUs in the Midwest to downwind Northeast sites. Although EGU NO_x emissions contribute only ~25% of NO_x emissions to the eastern U.S. (*33*), other stationary industrial NO_x sources contribute an additional ~15%; the strong correlations we observe may reflect the combined influence of these two stationary sources, especially given that many industrial sources use coal combustion to generate electricity.

The correlations between EGU NO_x emissions and $\delta^{15}N$ values are stronger than similar comparisons between EGU NO_x emissions and precipitation chemistry (e.g., NO_3^-, SO_4^{2-}, and pH concentrations) (Figure 3b). For example, r^2 values between $\delta^{15}N$ and EGU NO_x emissions within 640 km range from 0.67 to 0.78, whereas those for NO_3^-, SO_4^{2-}, and pH are on average about 30% lower. While nonlinearities that result from seasonal changes in oxidation rates and pathways, competition for oxidants, or removal processes may influence relationships between NO_x emissions and precipitation chemistry, these same processes may not necessarily affect $\delta^{15}N$ values. These comparisons suggest that $\delta^{15}N$ may be a

more robust indicator of the influence of surrounding stationary source NO_x emissions on precipitation monitoring sites than concentration and pH measurements alone and further highlight the potential utility of $\delta^{15}N$ values to trace NO_x sources. The strength of $\delta^{15}N$ as a tracer of EGU emissions is noteworthy because correlations between precipitation chemistry and regional emissions are widely used to assess the effectiveness of emission reduction strategies.

Temporal patterns in $\delta^{15}N$ values may result from seasonal changes in the relative proportions of NO_x sources that contribute to NO_3^- formation. Low summer $\delta^{15}N$ values may result from increased biogenic soil emissions and lightning during warmer months (*34*, *35*) that contribute NO_x with low $\delta^{15}N$ values. High winter $\delta^{15}N$ values generally correspond with peak winter EGU NO_x emissions, suggesting that seasonal $\delta^{15}N$ variations may also result from corresponding fluctuations in EGU NO_x emissions. For example, at the five sites characterized by the highest regional SO_4^{2-} concentrations, seasonal fluctuations in EGU NO_x emissions are significantly correlated with $\delta^{15}N$ values at four of the five sites ($0.67 < r^2 < 0.90$ and $p \leq 0.05$) (Supporting Information Figure SI-2). These results indicate that at NTN sites most affected by acidic deposition, temporal variations in $\delta^{15}N$ are correlated with seasonal variations in electricity generation and associated NO_x emissions.

Vehicle NO_x Emissions. In contrast to the strong correlations between $\delta^{15}N$ and stationary source emissions, county-level vehicle NO_x emissions, proportionally the largest emissions source in the eastern U.S. (54%) (*33*), are poorly correlated with $\delta^{15}N$ values during the same bimonthly periods ($0.14 < r^2 < 0.22$, $p < 0.05$, and $n = 33$ for all analyses) (Supporting Information Figure SI-3). These results are consistent with significant, positive correlations between NO_3^- and SO_4^{2-}concentrations in wet deposition for all bimonths ($0.54 < r^2 < 0.86$, $p < 0.001$, and $n = 33$ for all analyses) and together suggest a dominantly non-vehicle NO_x source of NO_3^- deposition since vehicles emit negligible SO_2 relative to coal combustion sources.

Several factors may contribute to the poor correlations between $\delta^{15}N$ values and vehicle NO_x. First, several studies have shown that dry N deposition from vehicle NO_x decreases within several hundred meters of busy highways (*27*, *28*). Second, ground-level emissions of tailpipe NO_x relative to smokestack NO_x emissions higher in the troposphere may result in different reaction pathways and scavenging efficiencies for vehicle NO_x. Additionally, emission factor models of vehicle NO_x emissions have significant uncertainty, including the U.S. EPA MOBILE data used for comparison in this study (*36*, *37*). Multiple comparisons of MOBILE emission factors with empirically observed NO_x concentrations indicate that MOBILE overestimates vehicle NO_x emissions (*37*). Finally, we reiterate that additional research is needed to clarify the $\delta^{15}N$ values associated with various NO_x sources. In particular, an earlier study reported that $\delta^{15}N$ of NO_x from vehicles without catalytic converters in South Africa varied from −13 to −2‰ (*8*), whereas other studies have reported positive $\delta^{15}N$ values (*10*−*12*). Factors such as load, emission controls, and combustion temperatures associated with fuel type may all influence resulting $\delta^{15}N$ values.

Seasonal and Spatial Variations in Tropospheric Nitrogen Oxide Processing. Variations in NO_x processing may also contribute to variations in $\delta^{15}N$ values. For example, less solar radiation during the winter results in a larger proportion of HNO_3 produced via the N_2O_5 pathway. In comparison, greater rates of photolytically produced OH during the summertime result in a larger proportion of HNO_3 produced via this pathway. This seasonality in oxidation pathways may also affect seasonal patterns we observe in $\delta^{15}N$ values. Equilibrium reactions between NO_2, NO_3, and N_2O_5 could result in higher $\delta^{15}N$ values in the more oxidized N species (*38*). The higher proportion of HNO_3 produced during the winter, coupled with the equilibrium reactions associated with N_2O_5, may contribute to the higher $\delta^{15}N$ values observed during the winter across the region. In contrast, the kinetics of the unidirectional oxidation of NO_2 via the OH radical during the summer would be expected to lower $\delta^{15}N$ values in the product (HNO_3) relative to the reactant (NO_2).

To explore whether equilibrium fractionations between oxidized N species could account for variations observed in $\delta^{15}N$ values, we examined NO_2 and O_3 concentrations in 2000 at seven rural/suburban air quality monitoring sites in the northeastern U.S. Monthly concentrations for April-November 2000 were calculated from mean hourly values (U.S. EPA Air Quality System, http://www.epa.gov/ttn/airs/airsaqs/, accessed February 1, 2006). Mean monthly O_3 concentrations were greater than NO_2 concentrations at all sites ($n = 48$) during April-November 2000, with the exception of 1 month at site 1. This analysis indicates that O_3 concentrations are generally greater than NO_2 concentrations across this region, and thus, equilibrium fractionations are likely not responsible for observed spatial and temporal trends in $\delta^{15}N$ values during April-November. However, because data are not available during the critical winter months, when O_3 concentrations are likely the lowest, we cannot conclusively rule this out as a factor contributing to higher $\delta^{15}N$ values during winter months.

In addition, spatial gradients in key atmospheric N species and associated variations in oxidized N processing may also influence $\delta^{15}N$ values. Brown et al. (*39*) documented a spatial gradient in N_2O_5 lifetime across the midwestern and northeastern U.S. and concluded that hydrolysis of nocturnally produced N_2O_5 is faster in Ohio and western Pennsylvania than in states further east. The primary control on N_2O_5 uptake is sulfate aerosol loading—which is higher in Ohio and western Pennsylvania than in more eastern states (*39*). These spatial variations in the nocturnal processing of NO_x may contribute to the higher $\delta^{15}N$ values observed in western parts of the study area. As another example, SO_2 oxidation is limited by the availability of OH radicals and other oxidizing agents (*40*). This interdependence and competition between NO_x and SO_2 for OH oxidants may affect $\delta^{15}N$ values. For example, less competition for OH oxidation in eastern states characterized by lower SO_2 concentrations could result in greater net NO_x oxidation during the daytime via OH and lower $\delta^{15}N$ values than in more western states with higher SO_2. However, because gas phase oxidization rates of NO_x are approximately 10 times faster than those of SO_2 (*40*), it cannot yet be concluded that the gradient in NO_x and SO_2 emissions and subsequent competition for oxidants plays a role in the observed gradient in $\delta^{15}N$ values.

In addition to the possibilities presented previously that atmospheric processing of nitrogen oxides may influence $\delta^{15}N$ values, other fractionating mechanisms, such as the dissociation and selective evaporation of low $^{14}N-HNO_3$ from aerosols or the selective removal of ^{15}N with rainfall intensity and transport, may fractionate $\delta^{15}N$ values. For example, low $\delta^{15}N-NO_3^-$ values observed in snow and snowpack in the Artic region have been attributed to the rainout of heavier $\delta^{15}N$ during transport (*41*, *42*). However, subsequent work suggests that mass-dependent kinetic or equilibrium fractionations during transport should also fractionate $\delta^{18}O-NO_3^-$ in the same manner as $\delta^{15}N$ (*43*); since highly depleted $\delta^{18}O$ values are not observed in the Artic (*44*), this fractionation pathway is not likely controlling $\delta^{15}N$ distributions. Clearly, further work is needed to determine how atmospheric processing of oxidized nitrogen influences $\delta^{15}N$ values. Although the potential effect of atmospheric reactions on $\delta^{15}N$ cannot be ruled out, the strong correlations between

$\delta^{15}N$ and EGU emissions suggest that if atmospheric reactions alter $\delta^{15}N$ values, they do not diminish the ability of $\delta^{15}N$ to trace stationary source NO_x emissions across regional scales.

Mixing Models. Limited understanding of mechanism(s) responsible for $\delta^{15}N$ fractionation between source and receptor prohibits the development of a mechanistic model in this study; however, mixing models can be used to estimate contributions of end-member sources (vehicle and stationary NO_x emissions) to individual NTN sites. However, the large range in $\delta^{15}N$ values reported for different NO_x end-member sources allows only a rough approximation of source partitioning. We undertook a series of conceptual exercises to further elucidate the relationships between emissions loads from major NO_x sources surrounding each site, their respective $\delta^{15}N$ values, and the resulting $\delta^{15}N$ of wet NO_3^- deposition at individual sites. A series of three model formulations, including assumptions, limitations, and results, are described in detail in the Supporting Information. Table SI-2 summarizes key parameters and results from each model. Figures SI-4 and SI-5 illustrate model results.

The models use only data from January-February to minimize the influence of natural NO_x sources, such as biogenic soil emissions and lightning. This simplification allows us to consider NO_x contributions from only stationary sources and vehicles. The models use emissions data and estimates as described in the Experimental Procedures. In Models 1 and 2, the mixing proportions are determined by NO_x emission inventory data; thus, these models test ideas about end-member source values and fractionations. In contrast, Model 3 calculates mixing proportions from each end-member source using molar N/S ratios and $\delta^{15}N$ values in sources and wet deposition. The models and other key differences are summarized as follows: Model 1: a two-source, mass-weighted isotopic mixing model that incorporates emissions loads, expressed as emission densities, from stationary and vehicular NO_x sources; Model 2: Model 1 with an additional term to account for apparent fractionation in stationary source NO_x during transport across the deposition gradient; and Model 3: two-source, N/S ratio-weighted isotopic mixing model that predicts source contributions using molar N/S ratios in emissions (NO_x/SO_2) and wet deposition (NO_3^-/SO_4^{2-}) rather than emissions inputs.

Models 1 and 2 demonstrate that emission loads alone cannot explain the spatial patterns we observe in $\delta^{15}N$ values of NO_3^- (Supporting Information Table SI-2 and Figures SI-4 and SI-5). These models illustrate that $\delta^{15}N$ variability is best reproduced ($r^2 = 0.34$ and $y = 0.48x + 0.46$) if (i) fractionation with distance from stationary source NO_x is considered (up to −8‰ for sites furthest from the source area) and (ii) $\delta^{15}N$ values for stationary and vehicular NO_x sources are in the lower portion of published ranges (e.g., +6 and −1.4‰ for stationary and vehicle NO_x, respectively). Further, Model 3 suggests that stationary source NO_x emissions are the dominant contributor (>90%) to NO_3^- formation and subsequent deposition at the study sites, even when employing a range of source N/S ratios and $\delta^{15}N$ values. The results from Model 3 contrast with emission inventory data that indicate NO_x emissions are roughly equivalent from stationary and vehicle NO_x sources (51 and 49%, respectively) in the areas surrounding the 33 sites during January-February (Supporting Information Table SI-2).

These model results provide an additional indication that the balance of inputs from emission inventories cannot explain the spatial variability observed in $\delta^{15}N$ values. This further suggests that fossil fuel combustion by vehicular and stationary sources do not equally contribute to NO_3^- deposition at these study sites. Moreover, the use of N/S ratios provides additional evidence that NO_3^- deposition at these NTN sites is dominated by stationary rather than vehicular NO_x emissions. However, to make definitive conclusions regarding source contributions at individual locations, additional research is needed to explicitly characterize source $\delta^{15}N$ values and fractionations of NO_x during atmospheric processing.

Implications

Our observations of regional $\delta^{15}N$ variability, coupled with the strong correlations we observe with stationary source NO_x emissions, illustrate that $\delta^{15}N$ of NO_3^- in wet deposition can be used as a tool for understanding the fate of NO_x emissions in the environment. Furthermore, we propose that $\delta^{15}N$ in precipitation NO_3^- can be used to monitor progress toward NO_x stationary source reduction goals. For example, Title IV of the U.S. Clean Air Act Amendments of 1990 requires reductions in annual emissions of NO_x from electric utilities, and more recently, the Clean Air Interstate Rule mandates a 61% reduction in interstate, long-range transport of NO_x from EGUs by 2015. The results presented here indicate that spatial and temporal patterns in $\delta^{15}N$ values are a strong complement to existing tools, including atmospheric transport models and precipitation chemistry, to assess progress toward these mandated goals.

Our results suggest that wet NO_3^- deposition at 33 NTN monitoring sites in the midwestern and northeastern U.S. is dominated by inputs of NO_x from power plants rather than vehicles, despite inventories that indicate vehicle emissions are the dominant NO_x source in the eastern U.S. These results suggest that due to siting requirements for NTN sites, large parts of the study region may receive atmospheric NO_y deposition inputs in excess of that indicated by NTN chemistry data alone, especially urban settings and areas near highways. Our findings emphasize the need to improve the characterization of N deposition patterns, especially in near-road and urban environments, and to better assess the environmental and ecological impacts of vehicle NO_x emissions and associated deposition. Finally, our results illustrate the value of long-term monitoring data of nitrogenous emissions and deposition and suggest that these national monitoring networks may need to expand to advance our understanding of source−receptor relationships.

Acknowledgments

This study was funded by the U.S. Geological Survey, the New York State Energy Research and Development Authority, and the Electric Power Research Institute. We gratefully acknowledge laboratory assistance from Rebecca Glatz, Steve Silva, Dan Doctor, Doug Choy, Cecily Chang, and John Radyk. We thank Thomas McMullen, Roy Huntley, and Laurel Driver of the U.S. EPA for providing emissions data. We appreciate the generosity of the NADP Central Analytical Lab in sharing archived precipitation samples. We thank Mark Nilles and Rick Carlton for their support and Neil Cape for sharing ideas. We thank two anonymous reviewers for their helpful comments on this manuscript.

Supporting Information Available

Five additional figures, two tables, descriptions of mixing models, results, and references. This material is available free of charge via the Internet at http://pubs.acs.org.

Literature Cited

(1) Galloway, J. N.; Dentener, F. J.; Capone, D. G.; Boyer, E. W.; Howarth, R. W.; Seitzinger, S. P.; Asner, G. P.; Cleveland, C. C.; Green, P. A.; Holland, E. A.; Karl, D. M.; Michaels, A. F.; Porter, J. H.; Townsend, A. R.; Vorosmarty, C. J. Nitrogen cycles: Past, present, and future. *Biogeochemistry* **2004**, *70*, 153−226.

(2) Vitousek, P. M.; Aber, J. D.; Howarth, R. W.; Likens, G. E.; Matson, P. A.; Schindler, D. W.; Schlesinger, W. H.; Tilman, D. G. Human

alteration of the global nitrogen cycle: Sources and consequences. *Ecol. Appl.* **1997**, *7*, 737−750.
(3) Wolfe, A. H.; Patz, J. A. Reactive nitrogen and human health: Acute and long-term implications. *Ambio* **2002**, *31*, 120−125.
(4) Ehhalt, D.; Prather, M.; Dentener, F.; Derwent, R.; Dlugokencky, E.; Holland, E.; Isaksen, I.; Katima, J.; Kirchhoff, V.; Matson, P.; Midgley, P.; Wang, M. Atmospheric chemistry and greenhouse gases. In *Climate Change 2001: The Scientific Basis. Contribution of Working Group I to the Third Assessment Report of the Intergovernmental Panel on Climate Change*; Houghton, J. T., Ding, Y., Griggs, D. J., Noguer, M., van der Linden, P. J., Dai, K., Maskell, K., Johnson, C. A., Eds.; Cambridge University Press: New York, 2001.
(5) Driscoll, C. T.; Lawrence, G. B.; Bulger, A. J.; Butler, T. J.; Cronan, C. S.; Eagar, C.; Lambert, K. F.; Likens, G. E.; Stoddard, J. L.; Weathers, K. C. Acidic deposition in the Northeastern United States: Sources and inputs, ecosystem effects, and management strategies. *Bioscience* **2001**, *51*, 180−198.
(6) Kahl, J. S. et al. Have U.S. surface waters responded to the 1990 Clean Air Act Amendments? *Environ. Sci. Technol.* **2004**, *38*, 484−490.
(7) Driscoll, C. T.; Whitall, D.; Aber, J.; Boyer, E.; Castro, M.; Cronan, C.; Goodale, C. L.; Groffman, P.; Hopkinson, C.; Lambert, K.; Lawrence, G.; Ollinger, S. Nitrogen pollution in the northeastern United States: Sources, effects, and management options. *Bioscience* **2003**, *53*, 357−374.
(8) Heaton, T. H. E. $^{15}N/^{14}N$ ratios of NO_x from vehicle engines and coal-fired power stations. *Tellus* **1990**, *42*, 304−307.
(9) Kiga, T.; Watanabe, S.; Yoshikawa, K.; Asano, K.; Okitsu, S.; Tsunogai, U.; Narukawa, K. In *Evaluation of NO_x Formation in Pulverized Coal Firing by Use of Nitrogen Isotope Ratios*, ASME 2000 International Joint Power Generation Conference, Miami Beach, FL, July 23−26, 2000; ASME: Miami Beach, FL, 2000.
(10) Ammann, M.; Siegwolf, R.; Pichlmayer, F.; Suter, M.; Saurer, M.; Brunold, C. Estimating the uptake of traffic-derived NO_2 from ^{15}N abundance in Norway spruce needles. *Oecologia* **1999**, *118*, 124−131.
(11) Moore, H. The isotopic composition of ammonia, nitrogen dioxide, and nitrate in the atmosphere. *Atmos. Environ.* **1977**, *11*, 1239−1243.
(12) Pearson, J.; Wells, D. M.; Seller, K. J.; Bennett, A.; Soares, A.; Woodall, J.; Ingrouille, M. J. Traffic exposure increases natural ^{15}N and heavy metal concentrations in mosses. *New Phytol.* **2000**, *147*, 317−326.
(13) Hoering, T. The Isotopic composition of ammonia and nitrate ion in rain. *Geochim. Cosmochim. Acta* **1957**, *12*, 97−102.
(14) Freyer, H. D. Seasonal variation of $^{15}N/^{14}N$ ratios in atmospheric nitrate species. *Tellus* **1991**, *43*, 30−44.
(15) Russell, K. M.; Galloway, J. N.; Macko, S. A.; Moody, J. L.; Scudlark, J. R. Sources of nitrogen in wet deposition to the Chesapeake Bay region. *Atmos. Environ.* **1998**, *32*, 2453−2465.
(16) Freyer, H. D.; Kobel, K.; Delmas, R. J.; Kley, D.; Legrand, M. R. First results of $^{15}N/^{14}N$ ratios in nitrate from alpine and polar ice cores. *Tellus* **1996**, *48*, 93−105.
(17) Hastings, M. G.; Sigman, D. M.; Steig, E. J. Glacial/interglacial changes in the isotopes of nitrate from the Greenland Ice Sheet Project 2 (GISP2) ice core. *Global Biogeochem. Cycles* **2005**, *19* GB4024.
(18) Kendall, C. Tracing nitrogen sources and cycling in catchments. In *Isotope Tracers in Catchment Hydrology*; Kendall, C., McDonnell, J. J., Eds.; Elsevier: Amsterdam, 1998.
(19) Silva, S. R.; Kendall, C.; Wilkison, D. H.; Ziegler, A. C.; Chang, C. C. Y.; Avanzino, R. J. A new method for collection of nitrate from fresh water and the analysis of nitrogen and oxygen isotope ratios. *J. Hydrol.* **2000**, *228*, 22−36.
(20) Casciotti, K. L.; Sigman, D. M.; Hastings, M. G.; Bohlke, J. K.; Hilkert, A. Measurement of the oxygen isotopic composition of nitrate in seawater and freshwater using the denitrifier method. *Anal. Chem.* **2002**, *74*, 4905−4912.
(21) Sigman, D. M.; Casciotti, K. L.; Andreani, M.; Barford, C.; Galanter, M.; Bohlke, J. K. A bacterial method for the nitrogen isotopic analysis of nitrate in seawater and freshwater. *Anal. Chem.* **2001**, *73*, 4145−4153.
(22) Theobald, D. M. Land-use dynamics beyond the American urban fringe. *Geogr. Rev.* **2001**, *91*, 544−564.
(23) National Atmospheric Deposition Program. *Instruction Manual: NADP/NTN Site Selection and Installation*; Illinois State Water Survey: Champaign, IL, 2001; p 45.
(24) National Atmospheric Deposition Program Central Analytical Lab. *Standard Operating Procedure for the Determination of Cl, NO_3, and SO_4 using Dionex DX-500 Ion Chromatography and Chromeleon Software*; SOP#IC01; Illinois State Water Survey: Champaign, IL, 2006.
(25) Coplen, T. B.; Bohke, J. K.; Casciotti, K. L. Using dual-bacterial denitrification to improve delta ^{15}N determinations of nitrates containing mass-independent ^{17}O. *Rapid Commun. Mass Spectrom.* **2004**, *18*, 245−250.
(26) Wankel, S. D.; Elliott, E. M.; Kendall, C. Mass-Independent Oxygen Isotope Fractionation of Atmospheric Nitrate, *Abstracts of the Sixth International Symposium on Applied Isotope Geochemistry*, Prague, Czech Republic, September 11−16, 2005; Novak, M., Ed.; International Association of Geochemistry and Cosmochemistry: Houston, TX, 2005.
(27) Cape, J. N.; Tang, Y. S.; van Dijk, N.; Love, L.; Sutton, M. A.; Palmer, S. C. F. Concentrations of ammonia and nitrogen dioxide at roadside verges and their contribution to nitrogen deposition. *Environ. Pollut.* **2004**, *132*, 469−478.
(28) Kirchner, M.; Jakobi, G.; Felcht, E.; Bernhardt, M.; Fischer, A. Elevated NH_3 and NO_2 air concentrations and nitrogen deposition rates in the vicinity of a highway in Southern Bavaria. *Atmos. Environ.* **2005**, *39*, 4531−4542.
(29) Butler, T. J.; Likens, G. E.; Vermeylen, F. M.; Stunder, B. J. B. The impact of changing nitrogen oxide emissions on wet and dry nitrogen deposition in the northeastern U.S. *Atmos. Environ.* **2005**, *39*, 4851−4862.
(30) Butler, T. J.; Likens, G. E.; Stunder, B. J. B. Regional-scale impacts of Phase I of the Clean Air Act Amendments in the U.S.: The relation between emissions and concentrations, both wet and dry. *Atmos. Environ.* **2001**, *35*, 1015−1028.
(31) Dutkiewicz, V. A.; Das, M.; Husain, L. The relationship between regional SO_2 emissions and downwind aerosol sulfate concentrations in the northeastern U.S. *Atmos. Environ.* **2000**, *34*, 1821−1832.
(32) Paerl, H. W.; Dennis, R. L.; Whitall, D. R. Atmospheric deposition of nitrogen: Implications for nutrient over-enrichment of coastal waters. *Estuaries* **2002**, *25*, 677−693.
(33) U.S. EPA. *1999 National Emission Inventory (NEI) Documentation and Data, Final Version 3.0*; Emissions Factor Inventory Group, Office of Air Quality Planning and Standards, U.S. EPA: Research Triangle Park, NC, 2004.
(34) Jaegle, L.; Steinberger, L.; Martin, R. V.; Chance, K. Global partitioning of NO_x sources using satellite observations: Relative roles of fossil fuel combustion, biomass burning, and soil emissions. *Faraday Discuss.* **2005**, *130*, 407−423.
(35) Zhang, R. Y.; Tie, X. X.; Bond, D. W. Impacts of anthropogenic and natural NO_x sources over the U.S. on tropospheric chemistry. *Proc. Natl. Acad. Sci. U.S.A.* **2003**, *100*, 1505−1509.
(36) Parrish, D. D. Critical evaluation of U.S. on-road vehicle emission inventories. *Atmos. Environ.* **2006**, *40*, 2288−2300.
(37) Singh, R. B.; Sloan, J. J. A high-resolution NO_x emission factor model for North American motor vehicles. *Atmos. Environ.* **2006**, *40*, 5214−5223.
(38) Freyer, H. D.; Kley, D.; Volz-Thomas, A.; Kobel, K. On the interactions of isotopic exchange processes with photochemical reactions in atmospheric oxides of nitrogen. *J. Geophys. Res., [Atmos.]* **1993**, *98*, 14791−14796.
(39) Brown, S. S.; Ryerson, T. B.; Wollny, A. G.; Brock, C. A.; Peltier, R.; Sullivan, A. P.; Weber, R. J.; Dube, W. P.; Trainer, M.; Meagher, J. F.; Fehsenfeld, F. C.; Ravishankara, A. R. Variability in nocturnal nitrogen oxide processing and its role in regional air quality. *Science (Washington, DC, U.S.)* **2006**, *311*, 67−70.
(40) Calvert, J. G.; Lazrus, A.; Kok, G. L.; Heikes, B. G.; Walega, J. G.; Lind, J.; Cantrell, C. A. Chemical mechanisms of acid generation in the tropopsphere. *Nature (London, U.K.)* **1985**, *317*, 27−35.
(41) Heaton, T. H. E.; Wynn, P.; Tye, A. M. Low $^{15}N/^{14}N$ ratios for nitrate in snow in the High Arctic (79 °N). *Atmos. Environ.* **2004**, *38*, 5611−5621.
(42) Wada, E.; Shibata, R.; Torri. ^{15}N abundance in Antarctica: Origin of soil nitrogen and ecological implications. *Nature (London, U.K.)* **1981**, *292*, 327−329.
(43) Michalski, G.; Bockheim, J. G.; Kendall, C.; Thiemens, M. Isotopic composition of Antarctic Dry Valley nitrate: Implications for NO_y sources and cycling in Antarctica. *Geophys. Res. Lett.* **2005**, *32*, L13817.
(44) Hastings, M. G.; Steig, E. J.; Sigman, D. M. Seasonal variations in N and O isotopes of nitrate in snow at Summit, Greenland: Implications for the study of nitrate in snow and ice cores. *J. Geophys. Res., [Atmos.]* **2004**, *109*, D20306.

Received for review April 16, 2007. Revised manuscript received August 9, 2007. Accepted August 22, 2007.

ES070898T